Effects of poloxamer additives on strength, injectability, and shape stability of beta-tricalcium phosphate cement modified using ball-milling

KIM Yeeun[a]*, UYAMA Emi[a], SEKINE Kazumitsu[a], KAWANO Fumiaki[b], and HAMADA Kenichi[a]

[a] Department of Biomaterials and Bioengineering, Tokushima University Graduate School of Biomedical Sciences, 3-18-15 Kuramoto, Tokushima 770-8504, Japan.

[b] Department of Comprehensive Dentistry, Tokushima University Graduate School of Biomedical Sciences, 3-18-15 Kuramoto, Tokushima 770-8504, Japan.

* Corresponding author. Tel.: +81 88 633 7333; fax: +81 88 633 9125.

E-mail address: yennykim9106@gmail.com

ABBREVIATIONS

β-TCP: beta-tricalcium phosphate, CPC: calcium phosphate cement, HA: Hydroxyapatite

Abstract

A new CPC was developed in this study using a β-TCP powder mechano-chemically modified by ball-milling. The prototype CPC exhibits excellent fluidity for easy injection into bone defects; however, there is a risk of leakage from the defects immediately after implantation due to its high fluidity. The addition of poloxamer, an inverse thermoresponsive gelling agent, into CPC optimizes the fluidity. At lower temperatures, it forms a sol and maintains good injectability, whereas at the human body temperature, it transforms to a gel, reducing the fluidity and risk of leakage. In this study, the effects of poloxamer addition of 3, 5, and 10 mass% on the injectability, shape stability, and strength of the prototype CPC were evaluated. The calculated injectability of the prototype CPC pastes containing three different poloxamer contents was higher than that of the CPC paste without poloxamer for 15 min at 37 °C. Furthermore, the shape stability immediately after injection of the three CPC pastes with poloxamer was higher than that of the CPC paste without poloxamer. After 1 week of storage at 37 °C, the compressive strength and diametral tensile strength of the CPC compacts containing 10 mass% poloxamer were similar to those of the CPC compact without poloxamer. Additionally, the CPC compacts containing 10 mass% poloxamer exhibited clear plastic deformation after fracture. These results indicate that the addition of poloxamer to the prototype CPC could reduce the risk of leakage from bone defects and improve the fracture toughness with maintaining the injectability and strength.

Keywords:

β–TCP; Calcium phosphate cement; Poloxamer 407; Injectability; Shape stability; Strength.

1. Introduction

Calcium phosphates in many different forms exhibit many advantages as biomedical materials, such as excellent biocompatibility, bioactivity, and osteoconductivity. In particular, calcium phosphate cements (CPCs) are attractive bone substitutes because of their high injectability into bone defects for minimally invasive bone repair. However, the strength of injectable CPCs is commonly insufficient; they also leak or migrate from the injected bone defects. Therefore, an improved strength and immediate and complete solidification of CPCs after implantation are required for wide-range clinical applications with long lifetimes and low risks. One of the most commonly used processes for improving the strength of CPC is to increase the mixing ratio of calcium phosphate powder to the CPC liquid (powder/liquid (P/L) ratio). An increase in the P/L ratio is also effective in accelerating CPC solidification; however, it reduces the injectability of the CPC paste before solidification. It has been reported that the mechano-chemical modification of CPC powder through a planetary ball-milling process exhibited simultaneous improvements in strength, injectability, and solidification (Bae et al., 2015; Gbureck et al., 2003; Kim et al., 2021); however, further improvement is required.

One of the commonly used strategies to accelerate the solidification of CPC pastes after injection is the mixing of CPC and additives, in particular, gelling agents such as gelatin, glycerol, collagen, and chitosan, for viscosity control (Vezenkova and Locs, 2022). The addition of gelatin to CPCs is known to improve solidification, injectability of cement paste, and mechanical properties of the set cement, and has been reported to accelerate the setting reaction (Bigi et al., 2004a, 2004b; Fujishiro et al., 2001; Maazouz et al., 2017; Shie et al., 2008). The addition of glycerol also greatly improved the injectability of the CPC paste; however, it increased the setting time and decreased the strength (Leroux et al., 1999). The addition of chitosan also improved the injectability and strength of CPCs; however, the effect was limited (Leroux et al., 1999). The concentration of citric acid solution as the liquid component in the CPC influences both mechanical properties and biocompatibility (Yokoyama et al., 2002). Although gelling agents have been widely added to CPCs, their effects are not satisfactory. One possible reason is that the above agents exhibited an increase in the CPC paste fluidity with an increasing temperature. Therefore, to achieve an adequate fluidity of the cement in the human body, the injection is required to be performed at a temperature

higher than that of the human body with a risk of thermally damaging the tissue. Otherwise, injecting at a temperature lower than that of the human body enhances the difficulty of injection due to insufficient fluidity.

In contrast, there are gelling agents exhibiting inverse thermoresponsive properties; they are a sol phase at lower temperatures and a gel phase at higher temperatures. The CPC paste, including gelling agents, can be injected into the human body at a lower temperature and will be heated immediately because of the human body temperature, losing the liquidity and lowering the risk of leakage. Poloxamer is the inverse thermoresponsive gelling agent of a tri-block copolymer consisting of a central hydrophobic polypropylene oxide (PPO) block flanked by two hydrophilic polyethylene oxide (PEO) blocks. With a temperature increase, the copolymer chains aggregate to form a micellar structure owing to the dehydration of the hydrophobic PPO blocks (Dumortier et al., 2006). It is widely utilized as a surfactant because of its amphiphilic nature (Nagarajan, 1999; Yu et al., 2012). Biomedical applications based on their excellent biocompatibility can be widely found in tissue engineering and cell encapsulation (Doğan et al., 2012; Matthew et al., 2002). Poloxamer is utilized as a pharmaceutical additive because of its low toxicity, promotion of solubilization, and metabolic stability (Lee et al., 2014a, 2014b). These applications suggest that the biotoxicity of poloxamer is acceptable for biomedical applications. Moreover, the authors found research utilizing poloxamer as a surfactant to produce nanostructured HA crystals (Ye et al., 2010, 2012). It was suggested that poloxamer additives possibly delayed the HA crystal growth speed but did not inhibit the full transformation to HA crystal (Maazouz et al., 2017). Based on the above advantages, the authors adopted poloxamer as a gelling agent for CPC in this study. Although there are many potential advantages, the authors could find only one study utilizing poloxamer as a CPC additive (Maazouz et al., 2017). In the above, alpha-tricalcium phosphate-based CPC containing 20 mass% poloxamer exhibited excellent injectability and shape stability; however, the strength of the set CPC was reduced from that of set CPC without poloxamer. The objective of this study was to investigate the effects of the poloxamer content on the strength, injectability, and shape stability of the beta-tricalcium phosphate (β-TCP)-based CPC developed by the authors.

2. Materials and methods

The specimen preparation processes in this study, except the poloxamer addition, mainly followed those of previous papers by the authors (Bae et al., 2015; Ida et al., 2017; Kim et al., 2021), and are summarized as follows.

2.1. Preparation of CPC

β-TCP powder (Taihei Chemical Industrial Co. Ltd., Osaka, Japan) was modified using a planetary ball mill (Pulverisette7, Fritsch, Idar-Oberstein, Germany) and 15 mm-diameter zirconia balls (*ditto*) to change the size distribution and crystallinity. Seven balls, β-TCP powder (8 g), and ethanol (4 mL of ethanol (99.5%)) were placed in a 45 ml-zirconia pot (*ditto*) and milled at approximately 1000 rpm (motor speed) for 24 h. The resulting powder (mβ-TCP powder) was then dried at 60 °C in an oven for more than 12 h.

To produce the two kinds of mixing solutions, $CaCl_2$ (Kento chemical Co. Inc., Tokyo, Japan) and NaH_2PO_4 (Wako Pure Chemical Industries, Ltd., Osaka, Japan) were mixed with distilled water to a concentration of 1.25 M and 0.75 M, respectively, and then filtrated using a PES syringe filter (0.45 μm pore size, 013045S-SFPES, AS ONE Corp., Osaka, Japan). The mβ-TCP powder was first mixed with the $CaCl_2$ solution for 5 min and then with the NaH_2PO_4 solution for 1 min. To clarify the effects of the poloxamer 407 (2 set of 101 blocks of PEO and 56 blocks of PPO, BASF, Ludwigshafen, Germany) content on the properties of CPC, it was mixed with the NaH_2PO_4 solution to a concentration of 0.03, 0.05, and 0.1 g/ml. The mixing ratio of CPC powder to $CaCl_2$ solution to NaH_2PO_4 solution (or mixed solution with poloxamer) was 5:1:1 (g/mL/mL), that is, the P/L ratio of the mixed pastes were 2.5 g/ml, and the total Ca/P ratio of the mixing liquid used in this study was 1.67. Hereafter the specimens without poloxamer, and with 0.03, 0.05, and 0.1 g/ml poloxamer are called mβ-TCP, pol-3, pol-5 and pol-10, respectively. The CPC paste was prepared on a glass slab using a stainless-steel (SUS) spatula.

2.2. Injectability

The injectability of the CPC paste is defined as its ability to extrude through a small hole in a syringe fitted with a long needle (Dorozhkin, 2013). Approximately 2.8 g of the paste was filled into a disposable syringe (2 mm inner-diameter opening, 12 mm inner-diameter body, and 10 mL inner volume (Terumo Syringe, Terumo Corp., Tokyo, Japan)) immediately after mixing and then stored in a refrigerator (7 °C) for 1 h to enhance the injectability at lower temperature. The syringes were removed from the refrigerator

and the injection test was started immediately at a temperature of 7 °C. Some syringes were placed in an incubator (37 °C) and stored for 1, 5, 15, 30, and 60 min. They were removed from the incubator and the injection test was started immediately on the assumption that the temperature was maintained at 37 °C.

The CPC paste was extruded using a universal testing machine and a load cell at a crosshead speed of 20 mm/min and a maximum force of 300 N. A maximum force of 300 N was selected as the typical maximum force exerted by a hand on a syringe plunger (Kim et al., 2013). The injectability was calculated using the following equation:

$$\text{Injectability (\%)} = \frac{W_{ext}}{W} \times 100 \quad (1)$$

where W_{ext} is the mass of the paste extruded from the syringe and W is the initial mass of the paste in the syringe before injection.

2.3. Mechanical properties evaluation

The compressive strength (CS) and diametral tensile strength (DTS) of the CPC compact were evaluated as a function of the poloxamer 407 concentration. To produce the test specimen, the cement paste was filled into silicone (Shin-Etsu Chemical Co. Ltd., KE-1300T) molds using a SUS spatula. To evaluate the wet strength (strength in the wet condition), the specimen was then stored at 37 °C and at a humidity of 100% for 1, 3, and 5 h in an incubator. To evaluate the dry strength (strength under dry conditions), the specimen was stored for one week in an incubator, followed by a dehydration process at 50 °C in an oven for 1 d. The dimensions of the mold for the CS specimens were 3 mm in diameter and 6 mm in height, while those for the DTS specimen were 6 mm in diameter and 4 mm in height. After drying, the dimensions of the specimens were determined using a digital caliper. The CS and DTS were evaluated using a universal testing machine (Autograph AGS-500A, Shimadzu Corp., Kyoto, Japan) and a 1 kN load cell (Type SLBL-1kN) at a crosshead speed of 10 mm/min. The CS and DTS were calculated using the following equations:

$$\text{CS} = \frac{F_{max}}{\pi \times (\frac{d}{2})^2} \quad (2)$$

$$\text{DTS} = \frac{2 \times F_{max}}{\pi \times d \times l} \quad (3)$$

where d is the specimen diameter, F_{max} is the failure load, and l is the length of the specimen.

2.4. Characterization of specimens

The phase constitution of the CPC compact after setting was analyzed using X-ray diffractometry

(XRD; MiniFlex, Rigaku Corp., Tokyo, Japan) at a step size of 0.1° with CuKα radiation at 30 kV and 15 mA. Data was collected in the 2θ range of 20°–60° in continuous mode with a scan speed of 0.1°/min.

To calculate the porosity of the compacts, the real volume (*Vr*) of the compact was measured using a gas pycnometer (AccuPyc 1330, Micromeritics Instrument, Norcross, GA, USA). The mass of the specimen (*M*) was measured using a microbalance after dehydration at 50 °C. The bulk density (D_b), solid density (D_s), and porosity (*P*) of the compacts were calculated using the following equations:

$$D_b = \frac{M}{\pi \times d^2 \times l} \quad (4)$$

$$D_s = \frac{M}{V_r} \quad (5)$$

$$P\ (\%) = \left(1 - \frac{D_b}{D_s}\right) \times 100 \quad (6)$$

The fracture surfaces of the DTS specimens were gold-coated using an ion-coating apparatus (Electron Microscopy IB-3, Eiko Engineering Co. Ltd., Tokyo, Japan) and then observed using scanning electron microscopy (SEM; JCM5700, JEOL Co. Ltd., Tokyo, Japan) and field-emission SEM (FE-SEM; S-4700, Hitachi High-Tech, Tokyo, Japan).

2.5. Statistical analysis

All data was statistically analyzed using the Steel-Dwass Test in the EZR software (Kanda, 2013) to compare the mean values of the different groups. The number of specimens (n) was 6, 10, or 12. Statistical significance was accepted at a confidence level of 0.05.

3. Results

3.1. Injectability and shape stability of CPC paste

Fig. 1 shows the injectability of the mβ-TCP, pol-3, pol-5, and pol-10 cement pastes under a maximum force of 300 N according to the different storage times at 37 °C. All cement pastes containing poloxamer exhibited an injectability higher than that of mβ-TCP up to 15 min, and then exhibited a drastic decrease in injectability to 30 min. Note that the mβ-TCP paste was injectable at 30 min, while injection of all the cement pastes containing poloxamer was impossible or difficult at 30 min.

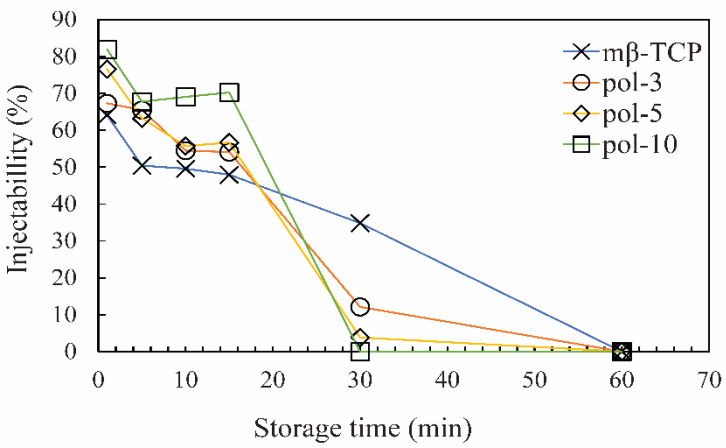

Fig. 1 Injectability of the mβ-TCP, pol-3, pol-5, and pol-10 cement pastes under a maximum force of 300 N according to different storage times at 37 °C

Fig. 2 shows optical images of the mβ-TCP, pol-3, pol-5, and pol-10 cement pastes injected after 10 min of storage at 37 °C. Although the injectability after 10 min of storage was the lowest, only the extruded mβ-TCP paste could not retain its injected shape, that is, the shape stability of the mβ-TCP paste was lower than that of the other pastes.

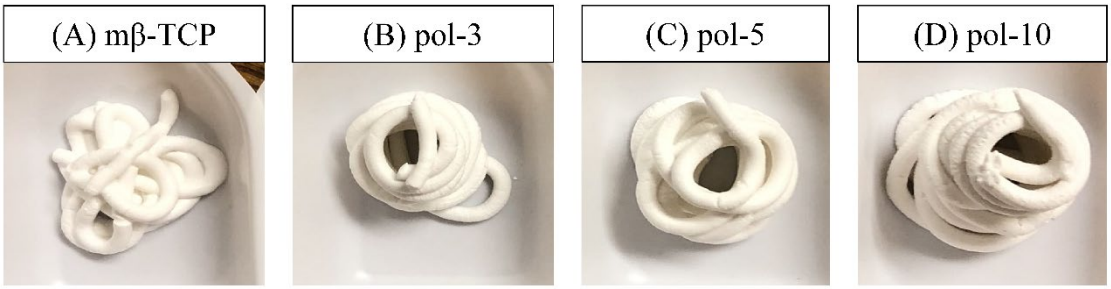

Fig. 2 Optical images of the mβ-TCP, pol-3, pol-5, and pol-10 cement pastes injected after 10 min of storage at 37 °C

3.2. Phase constitution and properties of the set cement

The XRD profiles of the mβ-TCP, pol-3, pol-5, and pol-10 crushed cement compacts after 1 week of storage are shown in Fig. 3. All the cement compacts, β-TCP, hydroxyapatite (HA), and zirconia (tetragonal zirconia (t-zr) and monoclinic zirconia (m-zr)) peaks could be observed in the patterns. The zirconia contaminations originated from the milling balls and milling pot (Kim et al., 2021).

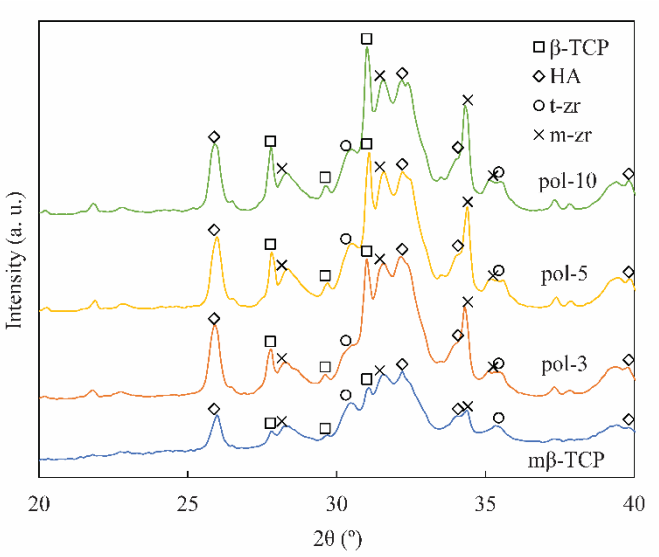

Fig. 3 XRD profiles of the crushed mβ-TCP, pol-3, pol-5, and pol-10 cement compacts after one week storage

Fig. 4 shows optical images of the pol-5 cement compacts after the DTS and CS evaluations after 5 h of storage at 37 °C. The specimens did not fracture into pieces and maintained the macroscopic form with a reduction in height, indicating that the pol-5 compact exhibited plastic deformation.

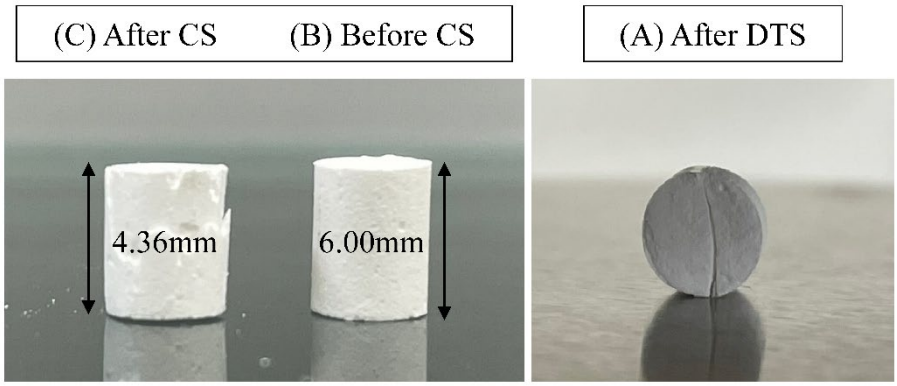

Fig. 4 Optical images of the pol-5 cement compacts (A) after the DTS evaluation, (B) and (C) before and after CS evaluation, respectively, after 5 h of storage

Fig. 5 shows the initial wet CS and DTS after 1, 3, and 5 h of storage. The mβ-TCP cement compacts exhibited an accelerated increase in the initial wet CS with an increasing storage time from 3 to 5 h, while they exhibited a gradual increase in the initial wet DTS values from 1 to 5 h of storage time. In contrast, the initial CS and DTS values of the pol-5 cement compacts did not increase from 3 to 5 h of storage time.

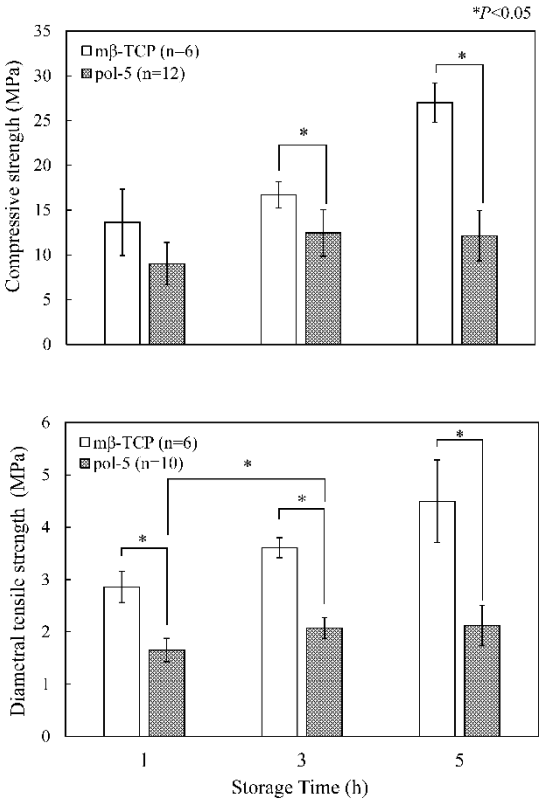

Fig. 5 CS and DTS of the cement compacts after 1, 3, and 5 h of storage

Fig. 6 shows the dry CS and DTS of the cement compacts after one week of storage. The CS values of the mβ-TCP, pol-3, pol-5, and pol-10 cement compacts were 37.9, 34.0, 37.4, and 35.4 MPa, respectively. The DTS values of the mβ-TCP, pol-3, pol-5, and pol-10 cement compacts were 5.0, 5.4, 5.1, and 4.9 MPa, respectively. The CS and DTS values of the cement compacts containing poloxamer were not significantly different from those of the mβ-TCP cement compacts.

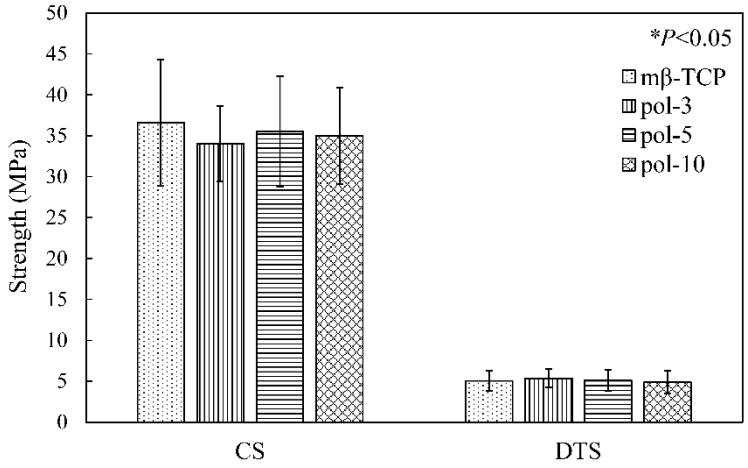

Fig. 6 CS and DTS of the cement compacts after one week of storage

Fig. 7 shows the porosity of the mβ-TCP, pol-3, pol-5, and pol-10 cement compacts. The porosity values were 44, 43, 45, and 46%, respectively. The porosity values were not significantly different.

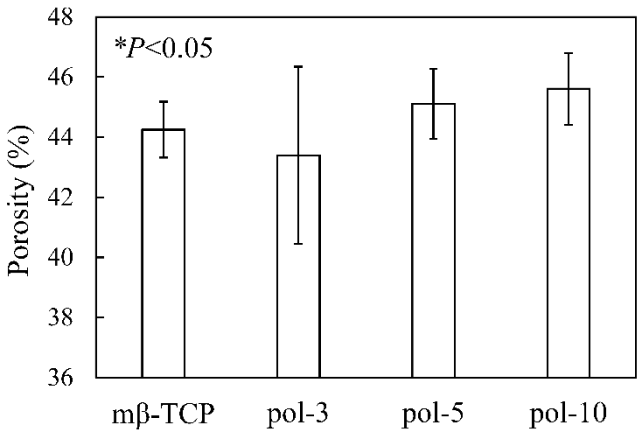

Fig. 7 The porosity of the mβ-TCP, pol-3, pol-5, and pol-10 cement compacts after one week of storage

3.3. Morphology of fracture surface of the cement compacts

Fig. 8 shows SEM images of the fracture surfaces of the DTS specimens after one week of storage. A highly developed needle-shaped or plate-shaped HA crystal network was observed on each fracture surface. Additionally, the size of the agglomerated granular structure of the HA crystals and the density of the larger pores on the fracture surface were similar. Fig. 9 shows FE-SEM images of the fracture surfaces of the DTS specimens after one week of storage. Entangled plate-shaped or needle-shaped crystals were observed on mβ-TCP and pol-10 of fracture surfaces.

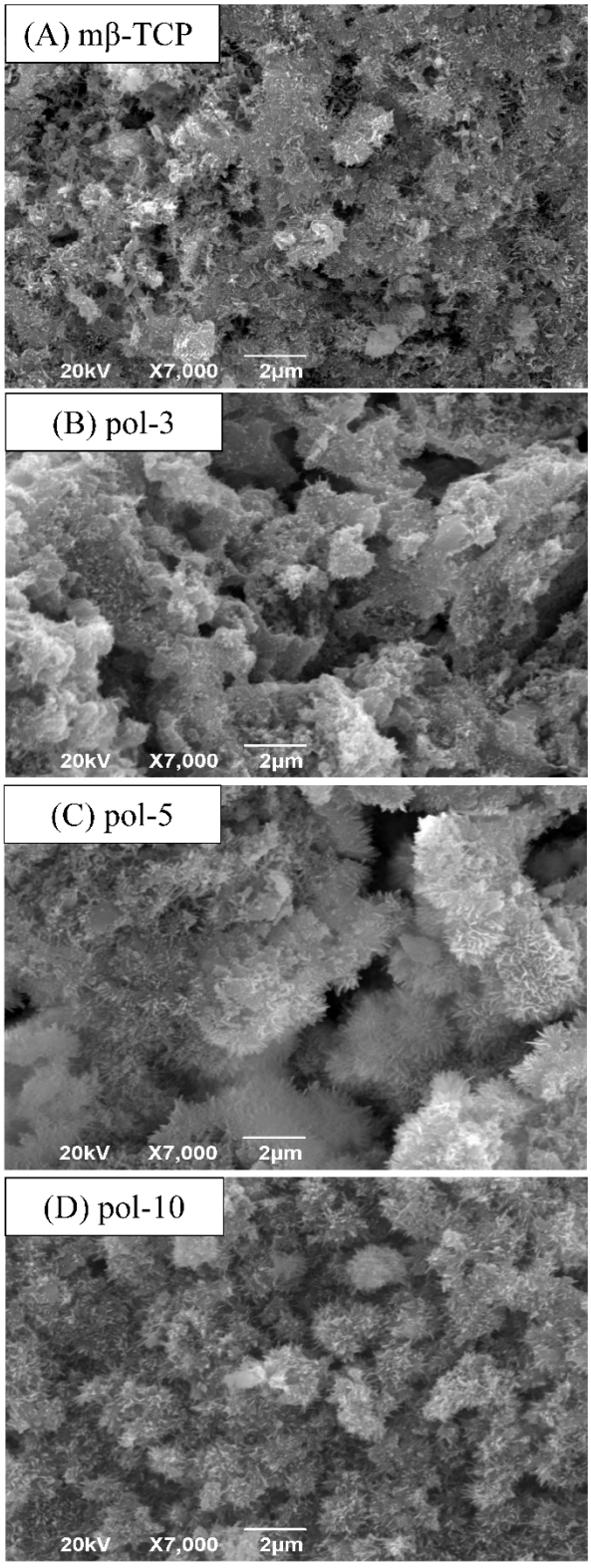

Fig. 8 SEM images of the fracture surfaces of DTS specimens after one week of storage

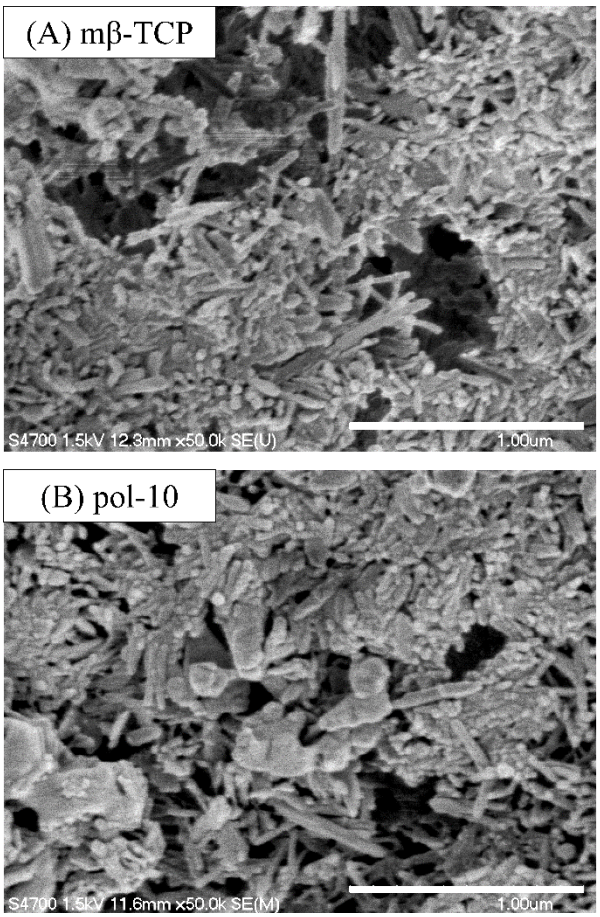

Fig. 9 FE-SEM images of the fracture surfaces of DTS specimens after one week of storage

4. Discussion

4.1. Injectability and shape stability of CPC paste

The mechanism responsible for the reduced injectability with increasing storage time, shown in Fig. 1, is either HA precipitation in the cement paste or the increase in the cement paste temperature in the syringe. The cement pastes containing poloxamer showed sufficiently high injectability before storage at 37 °C because the paste was at 7 °C and the poloxamer included was a sol. They drastically lost injectability due to the poloxamer transforming from a sol to a gel with an increasing temperature from 7 °C to 37 °C. In contrast, the injectability reduction of the mβ-TCP paste was gradual, as compared to that of the cement pastes containing poloxamer, due to the HA precipitation in the cement paste.

Fig. 2 shows that the injectability of the cement pastes evaluated in this study was different from the shape stability after injection. Although the cement pastes containing poloxamer exhibited a higher injectability than the mβ-TCP paste, they exhibited a nearly complete retention of their injected shape, that is, their shape stability at 37 °C was sufficiently high. Therefore, the addition of poloxamer provided the

cement paste with good injectability to bone defects and a low risk of leakage from bone defects.

In this study, the cement pastes containing poloxamer required more than 15 min to lose injectability, and the pastes could be injected up to 15 min after mixing. To extend the injectable time, if required, storage at a lower temperature is possibly effective, as suggested in a previous study (Maazouz et al., 2017).

4.2. Phase constitution of cement compacts

Poloxamer block copolymers exist as dissolved monomers in solution at lower temperatures, but they self-assemble as poloxamer micelles at higher temperatures (Huang et al., 2002). However, the presence of poloxamer could not be detected as a separate phase in the XRD profiles in this study. Therefore, it was concluded that the poloxamer addition in this study did not affect the crystal phase constitution of the cement compacts. Interestingly, the β-TCP peaks of pol-3, pol-5, and pol-10 were relatively higher than those of mβ-TCP, suggesting that the poloxamer addition suppressed the β-TCP dissolution. A lower β-TCP dissolution potentially led to less HA precipitation in the specimens. However, clear HA peaks could also be observed in pol-3, pol-5, and pol-10, suggesting that the poloxamer addition did not inhibit HA precipitation. These results are similar to the phenomenon reported in a previous study; that is, the addition of poloxamer delayed the HA crystal network growth during cement setting but did not delay the full transformation to HA (Maazouz et al., 2017). The mechanism for the inconsistent results of a lower β-TCP dissolution and clear HA precipitation could not be clarified in this study; however, the results of the set cement strength suggested that the HA crystal network was sufficiently developed after one week of storage.

4.3. Plastic deformability of cement compacts

The pol-5 cement compact after 5 h of storage exhibited excellent plastic deformability, as shown in Fig. 4. Generally, high plastic deformability leads to high fracture toughness; however, it is difficult for the authors to suggest the clinical advantages of high fracture toughness. One potential advantage is that the set cement in a bone defect can support the bone around the defect and reduce the risk of bone fracture. Another feature observed in Fig. 4 is the reduced release of small pieces after fracture. Small pieces released are at risk of migration outside the bone defect. Therefore, the addition of poloxamer can reduce the risk of leakage not only during injection, but also after setting.

4.4. Strength of cement compacts

Because the strength of poloxamer gel is lower than that of HA precipitates (Bercea et al., 2011; Ruys et al., 1995), the strength of the cement compacts will be discussed from the viewpoint of the HA crystal network growth in this section.

Because the set cement requires one day to dehydrate, the XRD profiles of the cement compact after 1, 3, and 5 h storage could not be obtained in this study. However, as the XRD profile after one week of storage indicated, the β-TCP dissolution was potentially also delayed, resulting in a delay in HA precipitation. Less HA precipitation leads to a lower HA crystal network growth and to lower CS and DTS values than mβ-TCP, as shown in Fig 5. In contrast, as shown in Fig. 6, the addition of less than 10% poloxamer did not decrease the CS and DTS of the cement compact after one week of storage. This result was consistent with that; that is, the HA precipitation in the cement compacts containing poloxamer after one week of storage was similar to or enhanced from that in the mβ-TCP cement compact, as the XRD profiles in Fig. 3 exhibited. The above results suggest that the poloxamer in the cement suppressed the dissolution of β-TCP; however, it simultaneously accelerated HA precipitation and growth of the HA network.

The less negative effect of the poloxamer addition on the cement compact strength in this study was different from the result of a previous study (Maazouz et al., 2017). The main reason for this difference could be the difference in poloxamer content (3% to 10% in this study and 20% in the previous study). Since HA precipitates and develops a network structure, a small amount of poloxamer is not an inhibitor of the HA crystal network growth. However, a higher poloxamer content delayed the HA crystal network growth, and the strength of the cement compacts was reduced. Therefore, it is believed that a poloxamer content of <10% did not affect the HA network growth in this study. And a 20% poloxamer content possibly reduced the growth as suggested in a previous study (Maazouz et al., 2017). A quantitative evaluation of the HA crystal network growth is required to further determine the effect of the poloxamer content on cement strength.

4.5. Porosity and morphology of the fracture surface of the cement compacts

Interestingly, there was no significant difference between the porosity of the cement compacts with and without poloxamer, that is, the poloxamer addition did not affect the porosity. Note that the volume of both the HA precipitation and poloxamer gel were measured as solid constitutions during the porosity evaluation, and because the contents of Ca and P included were constant, the volume of HA precipitated in

the cement was constant. Thus, the porosity of the cement compact depended only on the volume of the poloxamer. The water in the poloxamer gel was consumed for the generation of HA from β-TCP and was removed during dehydration. Thus, after dehydration, the poloxamer gel was transferred to a nearly xerogel and reduced its volume. This hypothesis suggests that a higher poloxamer content leads to higher porosity. However, the effect of the poloxamer content was not significant. A potential reason was that the difference in the poloxamer xerogel volume could not be detected in this study because the volume of the poloxamer xerogel contained was much smaller than that of the HA crystals. Although there was no significant difference in the average porosity value, the porosity distribution of the pol-3 cement compact was higher than those of the other cement compacts. However, the distribution of the pol-3 cement compact CS and DTS shown in Fig. 6 was similar to those of the other cement compacts. The mechanism of this inconsistency was not clarified in this study; however, one possible factor is the difference in pore size distribution because the strength of cement compacts depends on not only the porosity but also the pore size distribution and pore shape (Kim et al., 2021).

The observation of no clear difference between the fracture surfaces of the cements was inconsistent with the similar CS, DTS, and porosity. Interestingly, the poloxamer xerogel was not observed on the fracture surface, either because the content of poloxamer was significantly lower than that of the HA crystals or the structure of the poloxamer xerogel network was similar to the HA crystal network and could not be distinguished from one another.

5. Conclusions

The effects of 3, 5, and 10 mass% poloxamer addition on the properties of the prototype CPC using a modified β-TCP powder were evaluated. The addition exhibited the following effects:

1. The injectability of the prototype CPC stored for 15 min at 37 °C was similar or improved;
2. The shape stability after injection of the prototype CPC stored for 10 min at 37 °C was noticeably improved;
3. The CS and DTS of the prototype CPC containing 5 mass% poloxamer after 3 and 5 h of storage at 37 °C were significantly lower, while those after one week of storage at 37 °C and after 1 d of dehydration at 50 °C did not change significantly; and
4. The prototype CPC containing 5 mass% poloxamer after 5 h of storage at 37 °C exhibited obvious plastic deformation after the CS test.

These results indicate that a prototype CPC containing poloxamer with high injectability and low leakage risk after injection for minimally invasive surgery was successfully developed in this study.

Declaration of competing interests

The authors declare that they have no known competing financial interests or personal relationships that could have influenced the work reported in this study.

Acknowledgements

This study was partially supported by the Japan Society for the Promotion of Science (JSPS, KAKENHI Grant number 16K11626).

References

Bae, J., Ida, Y., Sekine, K., Kawano, F., Hamada, K., 2015. Effects of high-energy ball-milling on injectability and strength of β-tricalcium-phosphate cement. J. Mech. Behav. Biomed. Mater. 47, 77–86. https://doi.org/10.1016/J.JMBBM.2015.03.005.

Bercea, M., Darie, R.N., Niţă, L.E., Morariu, S., 2011. Temperature responsive gels based on pluronic F127 and poly(vinyl alcohol). Ind. Eng. Chem. Res. 50, 4199–4206. https://doi.org/10.1021/ie1024408.

Bigi, A., Bracci, B., Panzavolta, S., 2004a. Effect of added gelatin on the properties of calcium phosphate cement. Biomaterials. 25, 2893–2899. https://doi.org/10.1016/j.biomaterials.2003.09.059.

Bigi, A., Cantelli, I., Panzavolta, S., Rubini, K., 2004b. α-Tricalcium phosphate-gelatin composite cements. J. Appl. Biomater. Biomech. 2, 81–87. https://doi.org/10.1177/228080000400200203.

Doğan, A., Yalvaç, M.E., Şahin, F., Kabanov, A.V., Palotás, A., Rizvanov, A.A., 2012. Differentiation of human stem cells is promoted by amphiphilic pluronic block copolymers. Int. J. Nanomedicine. 7, 4849–4860. https://doi.org/10.2147/IJN.S31949.

Dorozhkin, S.V., 2013. Self-setting calcium orthophosphate formulations. J. Funct. Biomater. 4, 209–311. https://doi.org/10.3390/jfb4040209.

Dumortier, G., Grossiord, J.L., Agnely, F., Chaumeil, J.C., 2006. A review of poloxamer 407 pharmaceutical and pharmacological characteristics. Pharm. Res. 23, 2709–2728. https://doi.org/10.1007/s11095-006-9104-4.

Fujishiro, Y., Takahashi, K., Sato, T., 2001. Preparation and compressive strength of α-tricalcium phosphate/gelatin gel composite cement. J. Biomed. Mater. Res. 54, 525–530. https://doi.org/10.1002/1097-4636(20010315)54:4<525::aid-jbm80>3.0.co;2-#.

Gbureck, U., Grolms, O., Barralet, J.E., Grover, L.M., Thull, R., 2003. Mechanical activation and cement formation of β-tricalcium phosphate. Biomaterials24, 4123–4131. https://doi.org/10.1016/S0142-9612(03)00283-7.

Huang, K., Lee, B.P., Ingram, D.R., Messersmith, P.B., 2002. Synthesis and characterization of self-assembling block copolymers containing bioadhesive end groups. Biomacromolecules. 3, 397–406. https://doi.org/10.1021/bm015650p.

Ida, Y., Bae, J., Sekine, K., Kawano, F., Hamada, K., 2017. Effects of powder-to-liquid ratio on properties of β-tricalcium-phosphate cements modified using high-energy ball-milling. Dent. Mater. J. 36, 590–599. https://doi.org/10.4012/dmj.2016-341.

Kanda, Y., 2013. Investigation of the freely available easy-to-use software "EZR" for medical statistics. Bone Marrow Transplant. 48, 452–458. https://doi.org/10.1038/BMT.2012.244.

Kim, Y., Bae, J., Uyama, E., Sekine, K., Kawano, F., Hamada, K., 2021. Effects of zirconia additives on β-tricalcium-phosphate cement for high strength and high injectability. Ceram. Int. 47, 1882–1890. https://doi.org/10.1016/J.CERAMINT.2020.09.017.

Kim, Y.B., Lee, B.M., Lee, M.C., Noh, I., Lee, S.-J.J., Kim, S.S., 2013. Preparation and characterization of calcium phosphate cement of α-tricalcium phosphate-tetracalcium phosphate-dicalcium phosphate system incorporated with poly (γ-glutamic acid). Macromol. Res. 21, 892–898. https://doi.org/10.1007/S13233-013-1109-3.

Lee, J.H., Ryu, M.Y., Baek, H.R., Seo, J.H., Lee, K.M., Lee, J.H., 2014b. Generation of an rhBMP-2-loaded beta-tricalcium phosphate/hydrogel composite and evaluation of its efficacy on peri-implant bone formation. Biomed. Mater. 9, 055002. https://doi.org/10.1088/1748-6041/9/5/055002.

Lee, J.H., Baek, H.R., Lee, K.M., Lee, H.K., Im, S.B., Kim, Y.S., Lee, J.H., Chang, B.S., Lee, C.K., 2014a. The effect of poloxamer 407-based hydrogel on the osteoinductivity of demineralized bone matrix. Clin. Orthop. Surg. 6, 455–461. https://doi.org/10.4055/cios.2014.6.4.455.

Leroux, L., Hatim, Z., Frèche, M., Lacout, J.L., 1999. Effects of various adjuvants (lactic acid, glycerol, and chitosan) on the injectability of a calcium phosphate cement. Bone. 25 Supplement, 31S–34S. https://doi.org/10.1016/S8756-3282(99)00130-1.

Maazouz, Y., Montufar, E.B., Malbert, J., Espanol, M., Ginebra, M.P., 2017. Self-hardening and thermoresponsive alpha tricalcium phosphate/pluronic pastes. Acta Biomater. 49, 563–574. https://doi.org/10.1016/j.actbio.2016.11.043.

Matthew, J.E., Nazario, Y.L., Roberts, S.C., Bhatia, S.R., 2002. Effect of mammalian cell culture medium on the gelation properties of Pluronic® F127. Biomaterials. 23, 4615–4619. https://doi.org/10.1016/S0142-9612(02)00208-9.

Nagarajan, R., 1999. Solubilization of hydrocarbons and resulting aggregate shape transitions in aqueous solutions of Pluronic® (PEO-PPO-PEO) block copolymers. Colloids and Surfaces B: Biointerfaces. 16, 55–72. https://doi.org/10.1016/S0927-7765(99)00061-2.

Ruys, A.J., Wei, M., Sorrell, C.C., Dickson, M.R., Brandwood, A., Milthorpe, B.K., 1995. Sintering effects on the strength of hydroxyapatite. Biomaterials. 16, 409–415. https://doi.org/10.1016/0142-9612(95)98859-C.

Shie, M.Y., Chen, D.C.H., Wang, C.Y., Chiang, T.Y., Ding, S.J., 2008. Immersion behavior of gelatin-containing calcium phosphate cement. Acta Biomater. 4, 646–655. https://doi.org/10.1016/j.actbio.2007.10.011.

Vezenkova, A., Locs, J., 2022. Sudoku of porous, injectable calcium phosphate cements – Path to osteoinductivity. Bioactive Materials. https://doi.org/10.1016/j.bioactmat.2022.01.001.

Ye, F., Guo, H., Zhang, H., He, X., 2010. Polymeric micelle-templated synthesis of hydroxyapatite hollow nanoparticles for a drug delivery system. Acta Biomater. 6, 2212–2218. https://doi.org/10.1016/j.actbio.2009.12.014.

Ye, X., Cai, S., Xu, G., Dou, Y., Hu, H., 2012. Synthesis of mesoporous hydroxyapatite thin films using F127 as templates for biomedical applications. Mater. Lett. 85, 64–67. https://doi.org/10.1016/j.matlet.2012.07.001.

Yokoyama, A., Yamamoto, S., Kawasaki, T., Kohgo, T., Nakasu, M., 2002. Development of calcium phosphate cement using chitosan and citric acid for bone substitute materials. Biomaterials. 23, 1091–1101. https://doi.org/10.1016/S0142-9612(01)00221-6.

Yu, C.H., Lee, J.H., Baek, H.R., Nam, H., 2012. The effectiveness of poloxamer 407-based new anti-adhesive material in a laminectomy model in rats. Eur. Spine J. 21, 971–979. https://doi.org/10.1007/s00586-011-2098-6.